Appendix A – Details on Individual Tree-Ring Reconstructions and CMIP5 models

TR series code (see Table 1)	Brief description and specific original reference
North America	
NTR	MXD chronology: STD detrending – see D'Arrigo et al. (2004). RW data for this region used in DWJ06, not used for this location due to poor calibration.
GOA	RW based reconstruction: RCS detrending – see Wiles et al. (2014) – update of chronology used in DWJ06.
WRAx	MXD: STD detrending. Same version used in Wilson et al. (2007 – Appendix A) – original reference Davi et al. (2003). RW data for this region used in DWJ06, not used for this location due to poor calibration.
FIRT	MXD chronology: RCS-SF detrending – see Anchukaitis et al. (2013)
YUS	RW based reconstruction: STD detrending. Same version used in Wilson et al. (2007 – Appendix A) – original reference Youngblut and Luckman (2007)
YUN	RW based reconstruction: STD detrending. Same version used in Wilson et al. (2007 – Appendix A) – original reference Szeicz and MacDonald (1995)
IBC	RW, MXD and BI based reconstruction: STD detrending – see Wilson et al. (2014). BI - Blue Intensity is a relatively new tree-ring parameter (McCarroll et al. 2002; Campbell et al. 2011; Björklund et al. 2014; Rydval et al. 2014) that utilises the intensity of the reflectance of blue light of the TR latewood to derive an estimate of lignin content in latewood cells. As lignin content is reflected by density, raw BI and MXD are inversely correlated and both calibrate similarly to summer temperatures.
ICE	RW and MXD based reconstruction: RCS detrending – Same version used in DWJ06 – original reference Luckman and Wilson (2005)
IDA	RW based reconstruction: STD detrending. Same version used in Wilson et al. (2007 – Appendix A) – original reference Biondi et al. (1999)
COP	MXD chronology: RCS-SF detrending – see Anchukaitis et al. (2013)
THE	MXD chronology: RCS-SF detrending – see Anchukaitis et al. (2013)
QUEx	MXD chronology: RCS detrending – see Schneider et al. (2015). Period used for chronology is where replication ≥ 5 series.
QUEw	RW based reconstruction: RCS detrending – see Gennaretti et al. (2014).
NQU	RW composite chronology: STD detrending. Same version used in Wilson et al. (2007 – Appendix A) – original reference Payette (2007).
LAB	RW and MXD based reconstruction: RCS (RW), STD (MXD) detrending. RW data (D'Arrigo

	et al. 2003 – used in DWJ06) and MXD data (D'Arrigo et al. 2013) were combined using multiple-regression to derive a locally optimised calibration estimate of JJA temperatures.
Eurasia	
SCOT	RW and BI based reconstruction: RCS-SF detrending. Band-pass fusion of RW (low frequency) and BI (high frequency) – original reference Rydval et al. (submitted). For more information about BI, see IBC description above.
PYR	MXD based reconstruction: RCS detrending – see Dorado-Linan et al. (2012).
ALPS	MXD based reconstruction: RCS detrending - see Büntgen et al. (2006).
TYR	MXD chronology: RCS detrending – see Schneider et al. (2015). Period used for chronology is where replication ≥ 5 series.
JAEM	MXD based reconstruction: RCS detrending - see Zhang et al. (2015).
TAA	MXD composite chronology: RCS detrending – mean composite chronology of 3 chronologies (Tjeggelvas, Arjeplog and Ammarnäs). See Linderholm et al. (2014). Each composite chronology was normalised to z-scores over the period 1750-1950 and averaged while variance was stabilised to ensure no heteroscedasticity biases due to changing number of records using a modified equation from Osborn et al. (2007) – Appendix C1.
EFmean	MXD composite reconstruction: RCS detrending – mean of two northern Scandinavia studies to derive regional scale estimates of JJA mean temperatures. See Esper et al (2014) and Matskovsky and Helama (2014). These studies were used as they reflect, due to the high number of tree-ring records used, the most comprehensive compilation of available MXD data for this region. As they empirically could not be distinguished, a simple average of the two was made.
FORF	MXD chronology: RCS detrending – MXD data as used in McCarroll et al. (2013).
TAT	RW based reconstruction: RCS detrending – see Büntgen et al. (2013).
MOG	MXD based reconstruction: RCS detrending – see Klesse et al. (2014).
SFIN	MXD based reconstruction: RCS detrending – see Helama et al. (2014).
KOL	RW and BI reconstruction: RCS detrending. RW and BI chronologies were combined using multiple-regression to derive a locally optimised calibration estimate of JA temperatures. Original reference for data is McCarroll et al. (2013). For more information about BI, see IBC description above.
POLx	MXD chronology: RCS detrending – see Schneider et al. (2015). Period used for chronology is where replication ≥ 5 series.
YAM	RW chronology: RCS detrending – see Briffa et al. (2013).

ASGrid1	RW and MXD chronologies (varying weighting by grid): STD and RCS detrending. The 2x2 degree spatial resolution of the Cook et al. (2012) gridded reconstructions was reduced to create larger grid averages of 6 by 8 degrees (ca. 700-900 kms between grid centres - see Table 1). As the length of each 2x2 degree grid reconstruction varied, the final period used for each large grid average was where replication was ≥50% of the total number of small grids within each large grid region. Each 2x2 gridded reconstruction was normalised to z-scores over the period 1750-1950 and averaged while variance was stabilised to ensure no heteroscedasticity biases due to changing number of records using a modified equation from Osborn et al. (2007) – Appendix C1.
ASGrid2	See details for ASGrid1.
ASGrid10	See details for ASGrid1.
ASGrid11	See details for ASGrid1.
KYR	RW and MXD based reconstruction: STD detrending - Same version used in Wilson et al. (2007 – Appendix A).
MAN	MXD chronology: RCS detrending – see Schneider et al. (2015). Period used for chronology is where replication ≥ 5 series meaning that there is a gap from 1650-1673.
ASGrid3	See details for ASGrid1.
ASGrid12	See details for ASGrid1.
ALT	MXD chronology: RCS detrending – see Schneider et al. (2015). Period used for chronology is where replication ≥ 5 series.
ASGrid4	See details for ASGrid1.
ASGrid13	See details for ASGrid1.
OZN	RW based reconstruction: RCS detrending – see Davi et al. (2015)
TAY	RW chronology: RCS detrending - Same version used in DWJ06 – original reference Jacoby et al. (2000)
ASGrid5	See details for ASGrid1.
ASGrid14	See details for ASGrid1.
ASGrid6	See details for ASGrid1.
ASGrid15	See details for ASGrid1.
ASGrid7	See details for ASGrid1.
ASGrid16	See details for ASGrid1.
ASGrid8	See details for ASGrid1.
ASGrid17	See details for ASGrid1.
ASGrid9	See details for ASGrid1.

ASGrid18	See details for ASGrid1.
NJAP	RW and MXD based reconstruction: STD detrending – see D'Arrigo et al. (2014)
YAK	RW chronology: RCS detrending - Same version used in DWJ06 – original reference Hughes et al. (1999)

Appendix Table A1: Meta information for each chronology/reconstruction used for N-TREND2015.

Model	No. of Ens.	Solar	Volcanic	GHG	Land Use	Reference
BCC-CSM-1.1	1	Viera et al. (2011)	Gao et al. (2008)	Schmidt et al. (2012)	-	Wu et al (2013)
CCSM4	1	Viera et al. (2011)	Gao et al. (2008)	Schmidt et al. (2012)	Pongratz et al. (2008)	Landrum et al (2013)
GISS-E2-R 121	1	Steinhilber et al	Crowley and Unterman (2013)	Schmidt et al. (2012)	Pongratz et al. (2008)	Schmidt et al (2014)
GISS-E2-R 124	1	Viera et al. (2011)	Crowley and Unterman (2013)	Schmidt et al. (2012)	Pongratz et al. (2008)	Schmidt et al (2014)
GISS-E2-R 127	1	Viera et al. (2011)	Crowley and Unterman (2013)	Schmidt et al. (2012)	Kaplan et al. (2010)	Schmidt et al (2014)
FGOALS-gl	1	Crowley (2000)	Crowley (2000)	Amman et al. (2007)	-	Guo and Zhou (2013)
HadCM3	1	Steinhilber et al. (2009)	Crowley and Unterman (2013)	Schmidt et al. (2012)	Pongratz et al. (2008)	Schurer et al (2013)
MPI-ESM-P	3	Viera et al. (2011)	Crowley and Unterman (2013)	Schmidt et al. (2012)	Pongratz et al. (2008)	Jungclaus et al (2014)

Appendix Table A2: References for forcing information for each CMIP5 model.

Appendix B – Detailed calibration and validation nesting results and error estimation

			FULL calibration						Smoothed calibration		Early Calibration/Late Verification				Late Calibration/Early Verification				Early/Late Calibration/mid verification			
			1880-1988						20 yr spline: 1880-1988		1880-1934 vs 1935-1988				1935-1988 vs 1880-1934				1880-1915/1953-1988 vs 1916-1952			
Nest no.	Period	No. series	r2	DW	LinR	RMSE scaled best	RMSE additional	RMSE total	r2 SPL20	RMSE adjusted	Calr2	VerR2	VerRE	VerCE	Calr2	VerR2	VerRE	VerCE	Calr2	VerR2	VerRE	VerCE
BACK																						
1	1710-1988	54	0.41	1.88	-0.03	0.24	0.14	0.38	0.81	0.09	0.38	0.20	0.51	0.04	0.20	0.38	0.55	0.31	0.45	0.21	0.33	0.15
2	1689-1709	52	0.41	1.93	0.02	0.24	0.14	0.38	0.83	0.09	0.39	0.20	0.54	0.09	0.20	0.39	0.54	0.29	0.44	0.26	0.36	0.19
3	1684-1688	51	0.41	1.94	0.03	0.24	0.14	0.38	0.84	0.09	0.39	0.20	0.55	0.10	0.20	0.39	0.54	0.29	0.44	0.27	0.37	0.21
4	1642-1683	50	0.43	1.93	0.03	0.24	0.14	0.38	0.84	0.09	0.41	0.22	0.57	0.14	0.22	0.41	0.56	0.32	0.46	0.28	0.39	0.22
5	1640-1641	49	0.45	1.96	0.02	0.23	0.14	0.38	0.88	0.09	0.42	0.25	0.59	0.19	0.25	0.42	0.57	0.34	0.47	0.30	0.42	0.26
6	1638-1639	48	0.45	1.96	0.01	0.23	0.14	0.38	0.88	0.09	0.42	0.26	0.59	0.19	0.26	0.42	0.58	0.34	0.47	0.31	0.43	0.27
7	1600-1637	47	0.45	1.94	0.03	0.23	0.15	0.38	0.87	0.09	0.43	0.26	0.60	0.20	0.26	0.43	0.57	0.33	0.49	0.29	0.41	0.25
8	1593-1599	46	0.43	1.97	0.05	0.24	0.15	0.38	0.86	0.09	0.40	0.25	0.60	0.20	0.25	0.40	0.55	0.30	0.46	0.28	0.40	0.24
9	1551-1592	45	0.46	1.99	0.05	0.23	0.15	0.38	0.87	0.09	0.43	0.27	0.61	0.22	0.27	0.43	0.57	0.33	0.49	0.29	0.40	0.24
10	1521-1550	44	0.46	2.00	0.04	0.23	0.15	0.38	0.89	0.09	0.43	0.27	0.60	0.21	0.27	0.43	0.57	0.34	0.49	0.29	0.41	0.25
11	1510-1520	43	0.47	2.00	0.03	0.23	0.15	0.38	0.89	0.09	0.44	0.29	0.62	0.24	0.29	0.44	0.59	0.36	0.51	0.30	0.41	0.26
12	1492-1509	38	0.45	1.94	0.05	0.24	0.16	0.40	0.85	0.10	0.41	0.27	0.61	0.22	0.27	0.41	0.57	0.33	0.49	0.28	0.37	0.20
13	1396-1491	37	0.43	1.94	0.05	0.24	0.16	0.41	0.87	0.10	0.40	0.24	0.58	0.17	0.24	0.40	0.55	0.30	0.46	0.27	0.38	0.22
14	1373-1395	35	0.43	1.92	0.06	0.24	0.17	0.41	0.87	0.10	0.40	0.24	0.59	0.18	0.24	0.40	0.54	0.29	0.47	0.24	0.35	0.18
15	1342-1372	34	0.39	1.77	0.05	0.25	0.17	0.42	0.84	0.10	0.43	0.12	0.48	-0.04	0.12	0.43	0.46	0.16	0.44	0.19	0.28	0.09
16	1328-1341	33	0.39	1.76	0.04	0.25	0.17	0.43	0.84	0.10	0.43	0.12	0.47	-0.06	0.12	0.43	0.46	0.16	0.45	0.18	0.27	0.07
17	1260-1327	32	0.38	1.75	0.04	0.26	0.18	0.43	0.85	0.10	0.42	0.11	0.47	-0.05	0.11	0.42	0.45	0.15	0.43	0.19	0.28	0.09
18	1200-1259	31	0.40	1.77	0.03	0.25	0.18	0.43	0.86	0.10	0.43	0.12	0.47	-0.05	0.12	0.43	0.48	0.19	0.44	0.21	0.31	0.13
19	1135-1199	29	0.37	1.77	0.05	0.26	0.19	0.44	0.85	0.11	0.40	0.10	0.47	-0.05	0.10	0.40	0.44	0.12	0.41	0.20	0.32	0.13
20	1073-1134	28	0.33	1.69	0.03	0.26	0.19	0.45	0.80	0.11	0.38	0.06	0.39	-0.20	0.06	0.38	0.34	-0.02	0.37	0.15	0.26	0.06
21	1053-1072	27	0.29	1.64	0.08	0.27	0.19	0.47	0.80	0.12	0.34	0.04	0.39	-0.21	0.04	0.34	0.28	-0.12	0.34	0.12	0.23	0.03
22	1040-1052	26	0.30	1.64	0.08	0.27	0.20	0.47	0.80	0.12	0.33	0.04	0.40	-0.19	0.04	0.33	0.28	-0.11	0.34	0.12	0.22	0.01
23	1024-1039	25	0.30	1.67	0.09	0.27	0.20	0.47	0.82	0.12	0.34	0.05	0.41	-0.16	0.05	0.34	0.31	-0.08	0.35	0.13	0.24	0.04
24	978-1023	23	0.30	1.69	0.09	0.28	0.21	0.48	0.82	0.12	0.33	0.05	0.42	-0.14	0.05	0.33	0.31	-0.07	0.35	0.12	0.24	0.04
25	937-977	22	0.30	1.68	0.09	0.28	0.21	0.49	0.82	0.12	0.31	0.05	0.43	-0.12	0.05	0.31	0.31	-0.07	0.34	0.12	0.23	0.02
26	931-936	20	0.35	1.70	0.08	0.26	0.22	0.48	0.85	0.12	0.38	0.08	0.46	-0.08	0.08	0.38	0.38	0.04	0.38	0.17	0.32	0.13
27	918-930	19	0.34	1.70	0.09	0.26	0.23	0.49	0.86	0.12	0.37	0.08	0.45	-0.09	0.08	0.37	0.37	0.02	0.37	0.16	0.30	0.12
28	910-917	18	0.29	1.72	0.14	0.28	0.24	0.51	0.84	0.12	0.32	0.06	0.40	-0.18	0.06	0.32	0.29	-0.11	0.32	0.14	0.26	0.06
29	891-909	17	0.24	1.69	0.15	0.30	0.24	0.54	0.76	0.14	0.24	0.06	0.38	-0.23	0.06	0.24	0.26	-0.16	0.27	0.08	0.22	0.02
30	827-890	16	0.24	1.68	0.15	0.30	0.25	0.55	0.79	0.14	0.26	0.05	0.36	-0.27	0.05	0.26	0.24	-0.19	0.27	0.08	0.21	0.00
31	821-826	15	0.26	1.67	0.15	0.30	0.26	0.55	0.78	0.14	0.27	0.06	0.38	-0.23	0.06	0.27	0.27	-0.14	0.29	0.08	0.23	0.03
32	817-820	14	0.23	1.65	0.16	0.30	0.27	0.57	0.76	0.15	0.26	0.04	0.35	-0.30	0.04	0.26	0.23	-0.20	0.27	0.06	0.20	-0.02
33	800-1816	13	0.23	1.63	0.16	0.31	0.28	0.58	0.70	0.16	0.22	0.05	0.37	-0.25	0.05	0.22	0.24	-0.18	0.25	0.06	0.22	0.01
34	783-799	7	0.32	1.68	0.14	0.31	0.38	0.69	0.71	0.18	0.35	0.07	0.43	-0.13	0.07	0.35	0.33	-0.04	0.41	0.05	0.06	-0.19
35	760-782	6	0.29	1.69	0.17	0.31	0.41	0.72	0.71	0.19	0.32	0.06	0.40	-0.19	0.06	0.32	0.30	-0.09	0.37	0.03	0.10	-0.14
36	755-759	5	0.21	1.73	0.23	0.35	0.45	0.80	0.65	0.22	0.24	0.03	0.31	-0.37	0.03	0.24	0.18	-0.28	0.28	0.00	0.02	-0.24
37	750-754	4	0.21	1.76	0.19	0.38	0.50	0.88	0.67	0.24	0.21	0.02	0.34	-0.32	0.02	0.21	0.18	-0.27	0.27	0.01	0.09	-0.15
FORWARD																						
1	1989	52	0.38	1.78	-0.01	0.25	0.14	0.39	0.80	0.10	0.38	0.14	0.46	-0.07	0.14	0.38	0.50	0.23	0.44	0.17	0.26	0.06
2	1990	34	0.35	1.68	0.07	0.27	0.17	0.44	0.73	0.11	0.35	0.12	0.50	0.00	0.12	0.35	0.44	0.13	0.42	0.14	0.17	-0.05
3	1991-1992	33	0.34	1.68	0.07	0.27	0.17	0.44	0.73	0.12	0.33	0.11	0.51	0.02	0.11	0.33	0.44	0.12	0.40	0.14	0.17	-0.05
4	1993	31	0.35	1.64	0.05	0.27	0.18	0.45	0.71	0.12	0.33	0.11	0.51	0.03	0.11	0.33	0.44	0.14	0.41	0.13	0.19	-0.03
5	1994	30	0.34	1.65	0.05	0.27	0.18	0.45	0.72	0.12	0.32	0.11	0.51	0.02	0.11	0.32	0.44	0.12	0.38	0.15	0.26	0.07
6	1995	28	0.34	1.66	0.02	0.28	0.19	0.47	0.73	0.12	0.33	0.10	0.50	0.00	0.10	0.33	0.45	0.14	0.40	0.12	0.24	0.03
7	1996-1998	26	0.33	1.73	0.04	0.28	0.20	0.48	0.72	0.13	0.30	0.10	0.49	0.00	0.10	0.30	0.42	0.09	0.36	0.13	0.26	0.06
8	1999-2000	25	0.32	1.74	0.09	0.28	0.20	0.48	0.72	0.13	0.32	0.08	0.46	-0.07	0.08	0.32	0.37	0.02	0.33	0.17	0.31	0.13
9	2001	23	0.32	1.74	0.09	0.28	0.21	0.49	0.72	0.13	0.32	0.09	0.48	-0.04	0.09	0.32	0.38	0.04	0.34	0.17	0.31	0.13
10	2002	22	0.34	1.74	0.10	0.28	0.21	0.49	0.74	0.13	0.36	0.08	0.46	-0.07	0.08	0.36	0.38	0.04	0.37	0.17	0.28	0.09
11	2003	19	0.34	1.70	0.11	0.29	0.23	0.52	0.71	0.14	0.38	0.07	0.44	-0.12	0.07	0.38	0.36	0.01	0.37	0.14	0.30	0.12
12	2004	17	0.32	1.72	0.12	0.29	0.24	0.53	0.72	0.14	0.36	0.06	0.42	-0.15	0.06	0.36	0.33	-0.05	0.35	0.12	0.29	0.09
13	2005	15	0.25	1.69	0.13	0.31	0.26	0.57	0.73	0.15	0.29	0.01	0.36	-0.27	0.01	0.29	0.17	-0.29	0.28	0.06	0.22	0.01
14	2006	10	0.23	1.58	0.14	0.31	0.32	0.63	0.76	0.16	0.27	0.02	0.34	-0.31	0.02	0.27	0.18	-0.27	0.27	0.05	0.18	-0.04
15	2007	9	0.20	1.55	0.17	0.32	0.33	0.65	0.80	0.16	0.26	0.01	0.28	-0.42	0.01	0.26	0.11	-0.39	0.24	0.03	0.14	-0.09
16	2008-2010	8	0.20	1.53	0.17	0.32	0.35	0.67	0.79	0.17	0.25	0.02	0.31	-0.38	0.02	0.25	0.15	-0.33	0.24	0.04	0.15	-0.08
17	2011	3	0.13	1.36	0.24	0.33	0.58	0.91	0.23	0.42	0.17	0.00	0.25	-0.49	0.00	0.17	-0.03	-0.60	0.21	0.13	-0.15	-0.46

Appendix Table B1: Calibration and validation results for each nested model. R^2, square of the multiple correlation coefficient; DW, Durbin and Watson statistic for residual autocorrelation; Lin R, correlation of linear trend of residuals; RMSE, root-mean-square error; RE, reduction of error; CE, coefficient of efficienc. Red values denote non-significance for residual analysis and validation metrics.

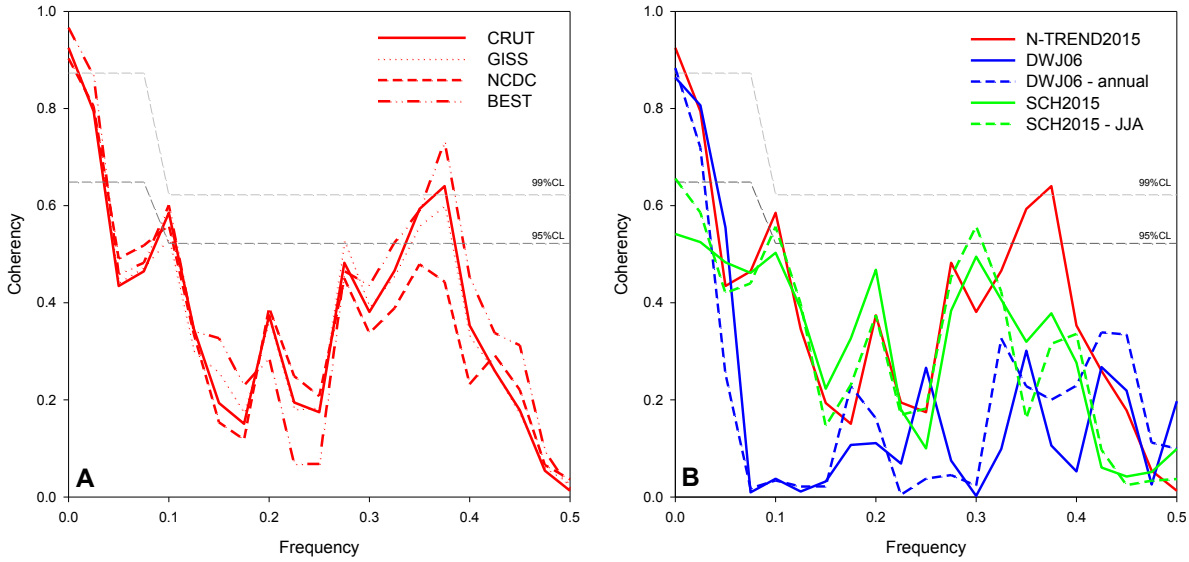

Appendix Figure B1: A: Coherency analysis (1880-1988) of N-TREND2015 with CRUT (Jones et al. 2012), GISS (Hansen et al. 2010), NCDC (Lawrimore et al. 2011) and BEST (Rohde et al. 2013) temperatures series for MJJA season; **B:** Coherency analysis (1880-1988) of N-TREND2015, DWJ06 and SCH2015 with CRUT3 mean May-August mean land-only temperatures (40-75°N). NB. DWJ06 was originally calibrated against annual temperatures and SCH2015 was optimally calibrated against JJA temperatures so these seasonal analyses are also shown.

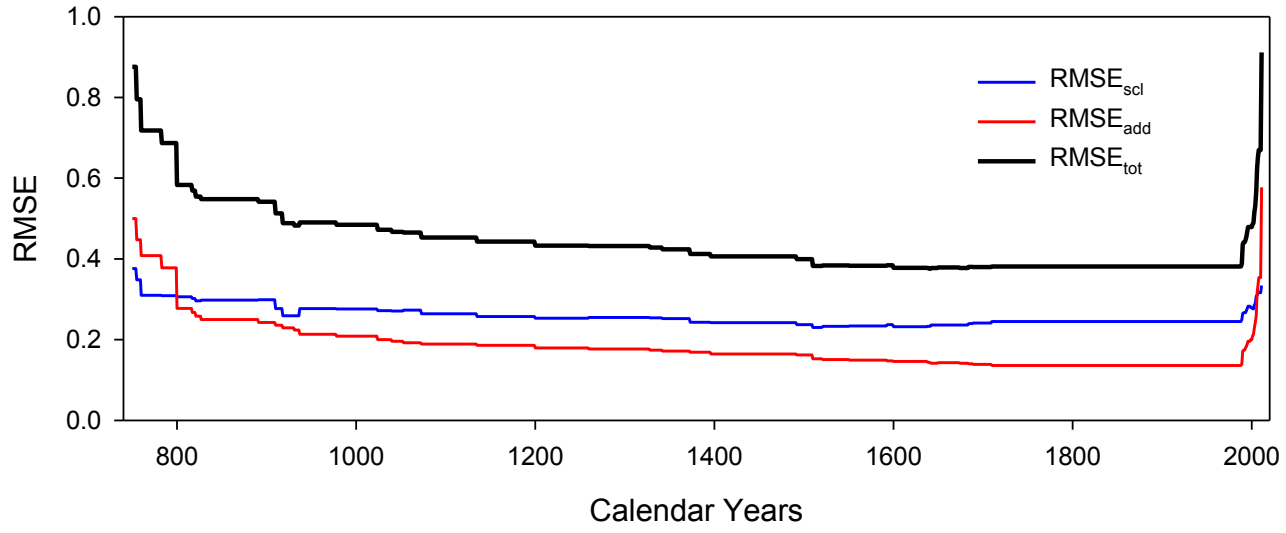

Appendix Figure B2: Non-smoothed RMSE estimates for each nest. Two error estimates were calculated. $RMSE_{scl}$ = the RMSE between each nest and NH MJJA mean temperatures after the nested series was scaled to NEST 1 over the 1710-1988 period; $RMSE_{add}$ = additional error related to the worst case scenario of a TR record expressing no signal with the local temperature data. This value is the grand mean RMSE value (divided by the square root of the number of records for each year) for all 54 locations if calibration r^2 was zero. $RMSE_{tot}$ = $RMSE_{scl}$ + $RMSE_{add}$, providing a more conservative estimate of uncertainty for the reconstruction.

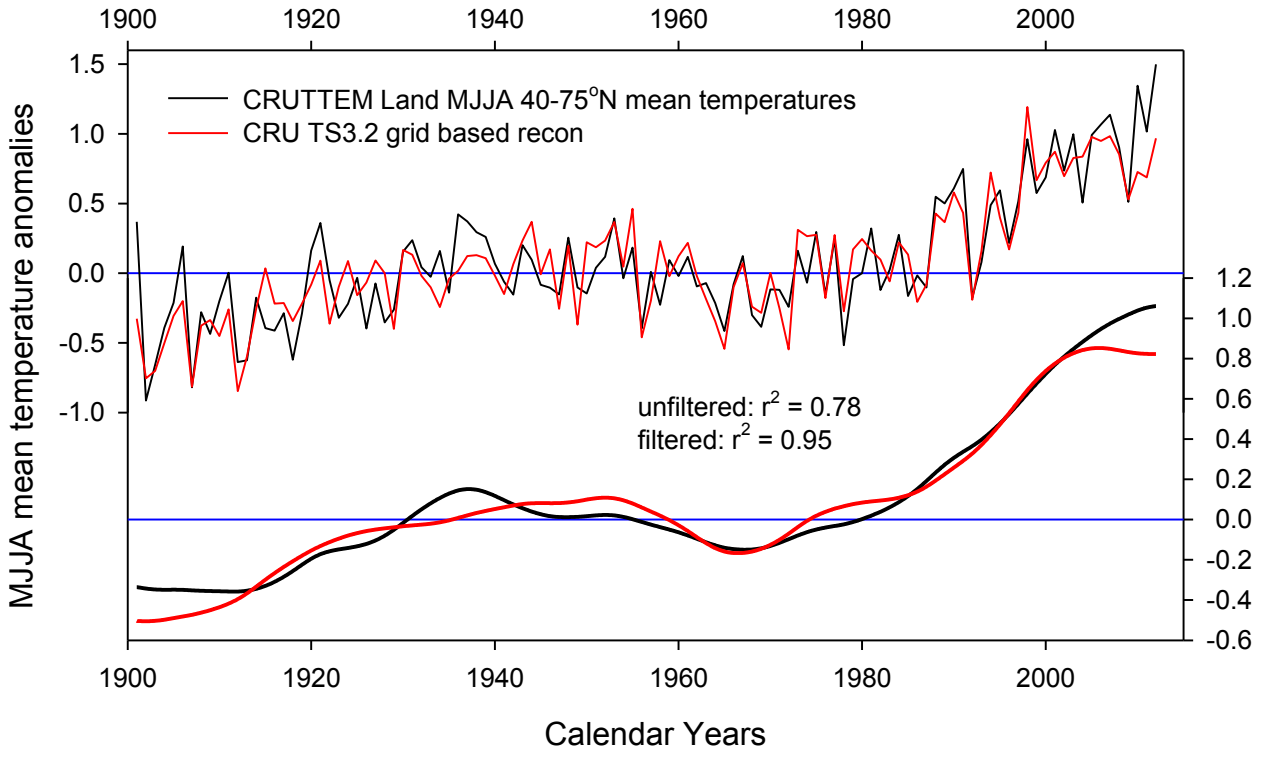

Appendix Figure B3: 54 Local gridded (CRUT3.2 - Harris et al. 2014) instrumental based NH reconstruction of CRUTEM (Jones et al. 2012) mean MJJA temperatures (40-75°N).

Appendix C – Reconstruction variant experiments with different methods and spatial weighting

To ascertain how sensitive the final N-TREND2015 reconstruction was to methodological options, a variety of different versions were derived using varying methodological approaches. For most of these experiments, the 54 input TR reconstructions were normalised to z-scores (mean = zero, standard deviation = 1) over the 1750-1950 period and averaged. As the number of records changes through time, the variance of the final mean composite series was adjusted using the following modified equation from Osborn et al. (1997):

$$Y(t) = X(t)\sqrt{\frac{n_t}{n_t(N)}} \qquad \text{Equation AC1}$$

where *Y(t)* is the variance stabilised estimate at year *t*, *X(t)* is the mean z-score value at year *t*, n_t is the number of records at year *t* and *N* is the total number of records for each composite variant.

Using this simple averaging plus variance stabilisation approach, it was possible to test a range of different methodological choices one could employ to derive a large scale NH composite series. Figure C1 presents an ensemble of different N-TREND2015 variants compared with the nested version detailed in the main text. The variants include: (1) simple mean of all data (no spatial weighting); (2) equal weighting between data from North America and Eurasia (2 quadrants). Figure C2 compares the continental composite series where strong inter-continental coherence is seen since the 1100s; (3) three quadrant version where Eurasia is divided into two quadrants and averaged equally with the North American data;

(4) equal weighting by dividing each continent into two (4 longitude quadrants). This is mathematically closest to the nesting method detailed in main text and the four regional series are shown in Figure C3; (5) equal weighting between high (57-72N) and low (40-57N) latitude and between both continent masses. The resultant high and low latitude composite series are compared in Figure C4; (6) weighting specifically by the different TR parameter (RW, MXD and mixed). The three different parameter composites are compared in Figure 7; (7) 4 quadrant weighting (option 4 above) but excluding the Asia2K (Cook et al. 2012) data; (8) 4 quadrant weighting (option 4 above) but data were smoothed with a 20-year spline before compositing; (9) Total least squares regression - following Hegerl et al 2007. This used 4 quadrants as in option 4, weighted by correlation over the calibration period (1880-1988). The reconstruction was split into 3 nested time periods 937-1988, 1073-1988, 1396-1988 and only tree-ring records that covered the whole periods used. The three time-series were then regressed onto the observations using a total least squares regression assuming a ratio of errors in the proxy reconstruction to instrumental ranging from 2 to 14, with an F-test used to calculate the likelihood of the residual. The best fit regression value was chosen as the one given by the noise ratio leading to the best likelihood (optimum noise ratio for the tree time periods: 6, 4, 3 respectively) and the three time-series combined; (10) area weighted mean of the gridded reconstructions from Part II, Anchukaitis et al. (in prep).

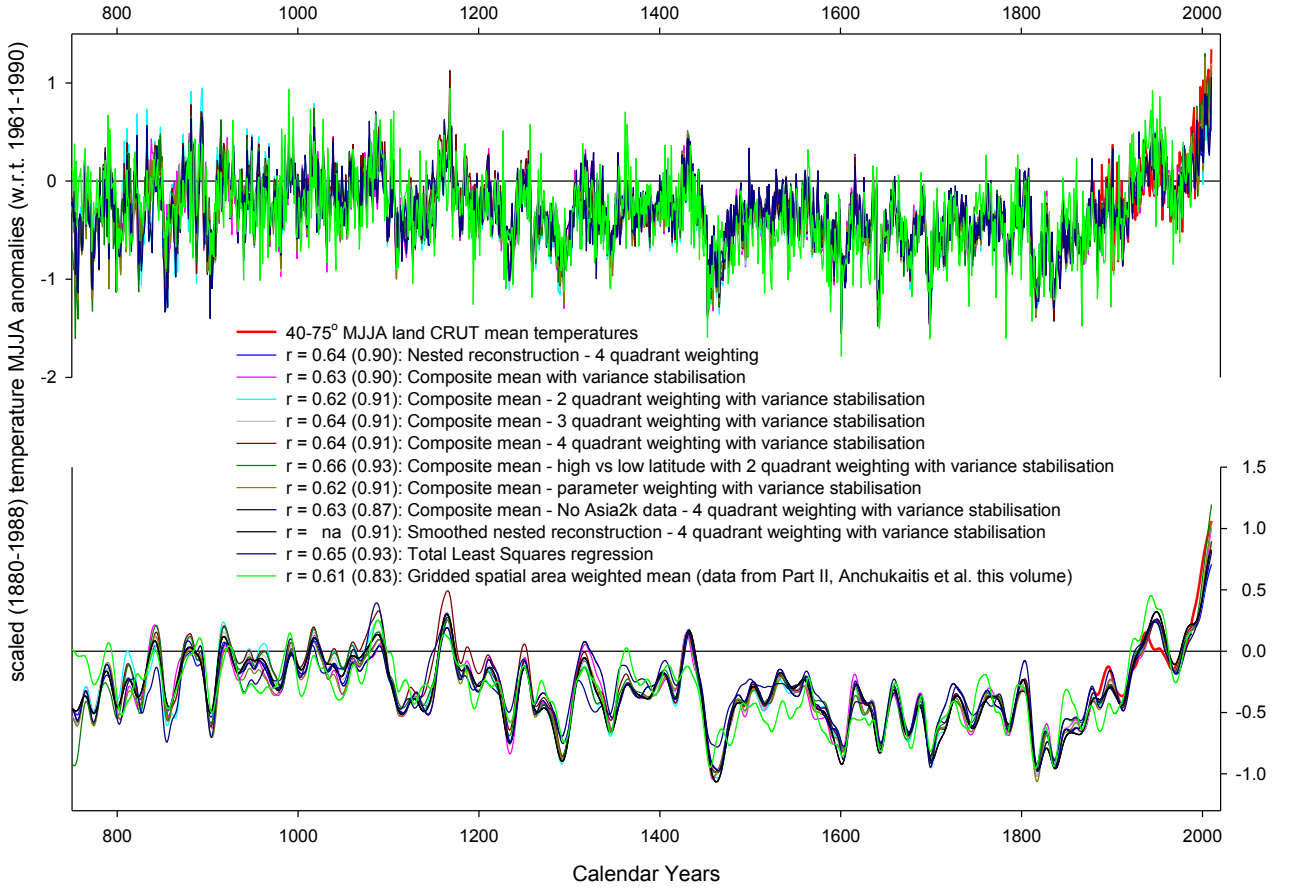

Appendix Figure C1: Variety of reconstruction variants focussing on different approaches to weigh the individual proxy records. Correlations (1880-1988) between each variant and NH CRUT MJJA mean temperatures are shown for non-transformed (and 20-year spline smoothed) versions. The gridded spatial mean (Anchukaitis et al. *in prep*) is not scaled to the 1880-1988 period.

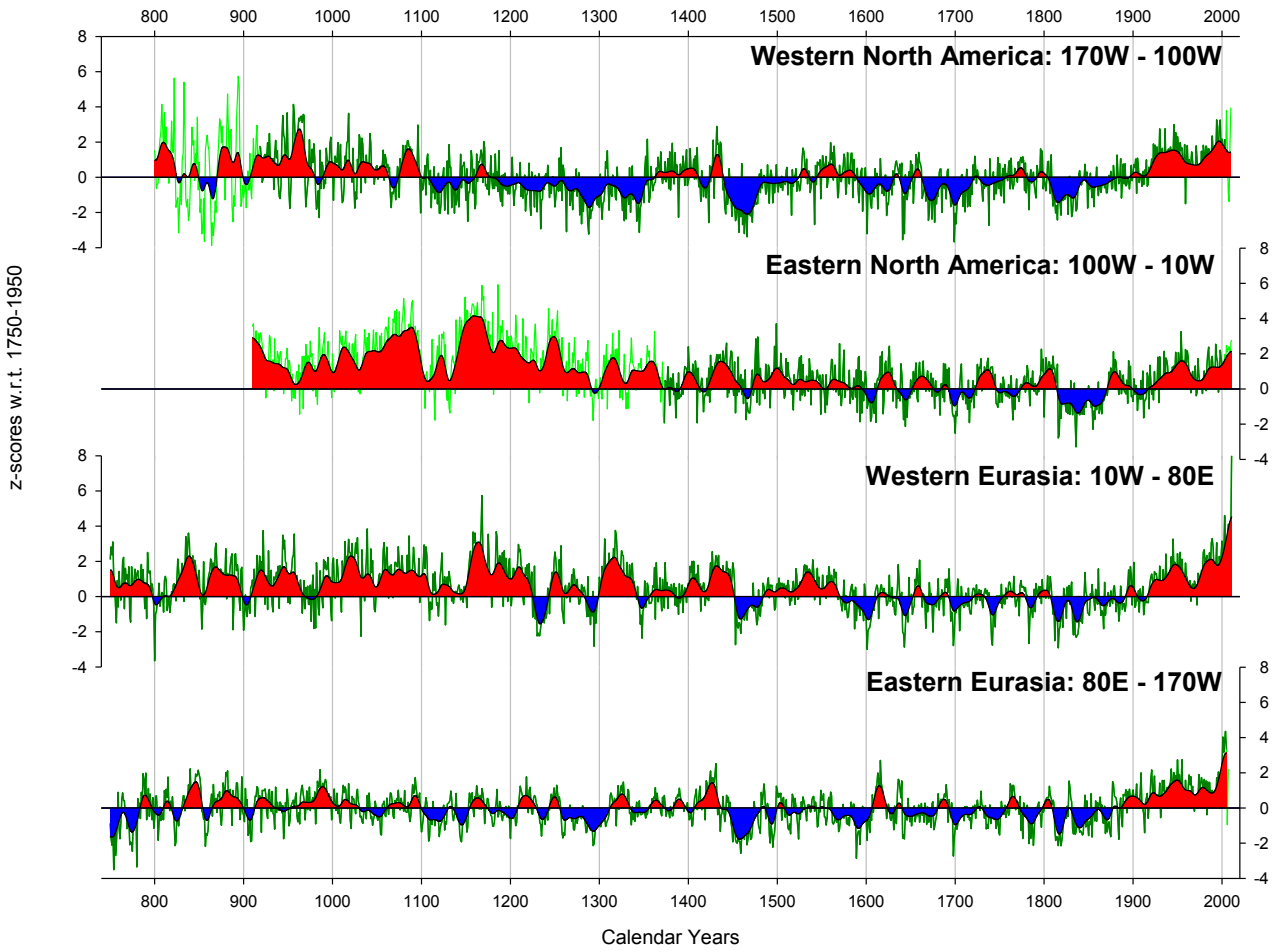

Appendix Figure C2: Longitude quadrant composite mean series. Light green highlighting denotes periods where TR series replication is < 3 records.

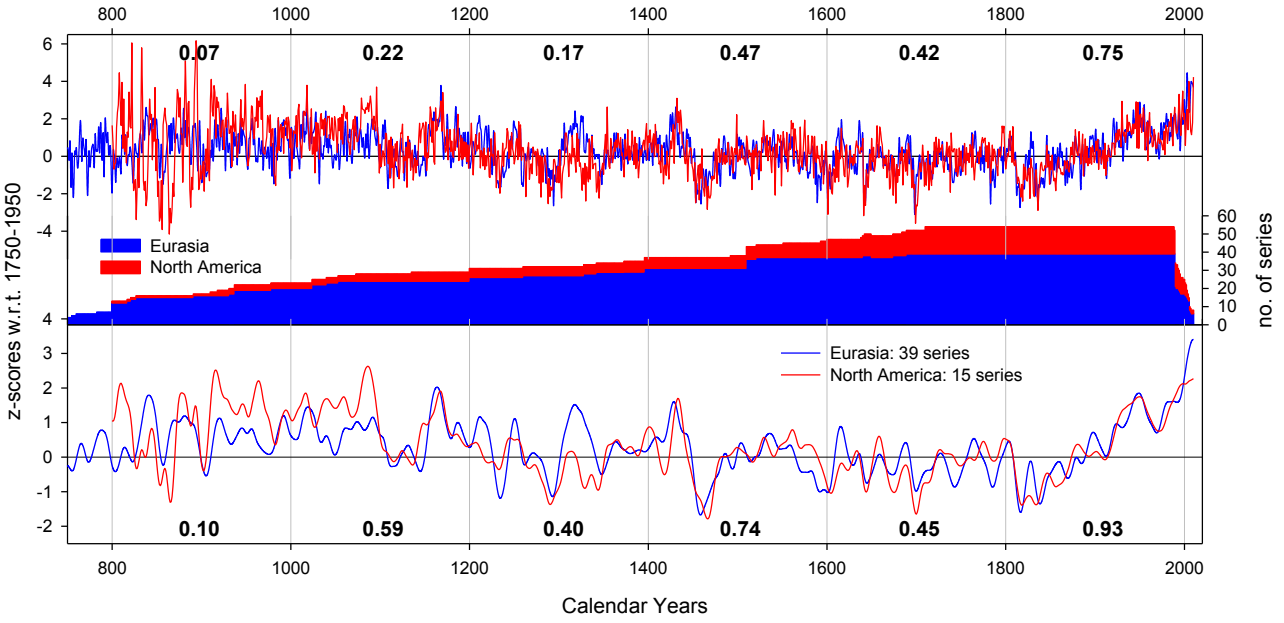

Appendix Figure C3: Comparison of North American and Eurasian composite mean series. Data are expressed as Z-score relative to the 1750-1950 period. Upper (lower) panel are unfiltered (filtered – 20-year spline) versions. Numerical values in upper and lower panels show correlations between the EU and NA unfiltered and filtered series for 200-year blocks.

Appendix References

Ammann, C., Joos, F., Schimel, D., Otto-Bliesner, B., Tomas, R., 2007. Solar influence on climate during the past millennium: results from transient simulations with the NCAR climate system Model. Proc. Natl. Acad. Sci. U.S.A. 104 (10), 3713-3718.

Crowley, T., 2000. Causes of climate change over the past 1000 years. Science 289 (5477), 270-277. http://dx.doi.org/10.1126/science.289.5477.270

Crowley, T.J., Unterman, M.B., 2013. Technical details concerning development of a 1200 yr proxy index for global volcanism. Earth System Science Data 5, 187–197, doi:10.5194/essd-5-187-2013.

Gao, C., Robock, A., Ammann, C., 2008. Volcanic forcing of climate over the past 1500 years: an improved ice core-based index for climate models. J. Geophys. Res. 113 http://dx.doi.org/10.1029/2008JD010239.

Guo, Z., Zhou, T., 2013. Why does FGOALS-gl reproduce a weak Medieval warm period but a reasonable Little Ice Age and 20th century warming? Adv. Atmos. Sci. 30 (6), 1758-1770. http://dx.doi.org/10.1007/s00376-013-2227-8

Hansen, J., Ruedy, R., Sato, M., Lo, K., 2010. Global surface temperature change. Reviews of Geophysics 48(4), RG4004, doi:10.1029/2010RG000345

Kaplan, J., Krumhardt, K., Ellis, E., Ruddiman, W., Lemmen, C., and Goldewijk, K., 2010. Holocene carbon emissions as a result of anthropogenic land cover change. Holocene, 21(5), 775–791. http://doi.org/10.1177/0959683610386983

Landrum, L., Otto-Bliesner, B. L., Wahl, E. R., Conley, A., Lawrence, P. , Rosenbloom, N., & Teng, H., 2013. Last Millennium Climate and Its Variability in CCSM4. Journal of Climate, 26(4), 1085–1111. http://doi.org/10.1175/JCLI-D-11-00326.1

Lawrimore, J., Menne, M., Gleason, B., Williams, C., Wuertz, D., Vose, R., Rennie, J., 2011. An overview of the Global Historical Climatology Network monthly mean temperature data set, version 3. Journal of Geophysical Research: Atmospheres (1984-2012) 116, D19121, doi:10.1029/2011JD016187

Pongratz, J., Reick, C., Raddatz, T., and Claussen, M., 2008. A reconstruction of global agricultural areas and land cover for the last millennium. Global and Biogeochemical Cycles, 22(3), n/a–n/a. http://doi.org/10.1029/2007GB003153

Rohde, R., Muller, R., Jacobsen, R., Muller, E., Perlmutter, S., Rosenfeld, A., Wurtele, J., Groom, D., Wickham, C., 2013. A New Estimate of the Average Earth Surface Land Temperature Spanning 1753 to 2011. Geoinformatics & Geostatistics: An Overview 1:1, doi:10.4172/gigs.1000101

Schmidt, G. , Jungclaus, J., Ammann, C. , Bard, E., Braconnot, P., Crowley, T., Vieira, L., 2012. Climate forcing reconstructions for use in PMIP simulations of the Last Millennium (v1.1).Geoscientific Model Development., 5(1), 185-191. doi:10.5194/gmd-5-185-2012

Schmidt, G., Kelley, M., Nazarenko, L., Ruedy, R., Russell, G. L., Aleinov, I., … Zhang, J., 2014. Configuration and assessment of the GISS ModelE2 contributions to the CMIP5 archive. Journal of Advances in Modeling Earth Systems, 6(1), 141–184. http://doi.org/10.1002/2013MS000265

Schurer, A. , Hegerl, G. , Mann, M. , Tett, S. F, Phipps, S. , 2013. Separating Forced from Chaotic Climate Variability over the Past Millennium. Journal of Climate, 26(18), 6954–6973. http://doi.org/10.1175/JCLI-D-12-00826.1

Steinhilber, F., Beer, J., & Fröhlich, C., 2009. Total solar irradiance during the Holocene. Geophysical Research Letters, 36(19), L19704. http://doi.org/10.1029/2009GL040142

Vieira, L. , Solanki, S., Krivova, N. , & Usoskin, I., 2011. Evolution of the solar irradiance during the Holocene. Astronomy & Astrophysics, 531, A6. http://doi.org/10.1051/0004-6361/201015843

Wu, T., Li, W., Ji, J., Xin, X., Li, L., Wang, Z., Zhang, Y., Li, J., Zhang, F., and Wei, M.,2013. Global carbon budgets simulated by the Beijing Climate Center Climate System Model for the last century. J. Geophys. Res.: Atm., 118(10), 4326–4347. http://doi.org/10.1002/jgrd.5032